

Spin Polaron Theory for the Photoemission Spectra of Layered Cobaltates

Jiří Chaloupka^{1,2} and Giniyat Khaliullin¹

¹Max-Planck-Institut für Festkörperforschung, Heisenbergstrasse 1, D-70569 Stuttgart, Germany

²Department of Condensed Matter Physics, Masaryk University, Kotlářská 2, 61137 Brno, Czech Republic

(Received 3 August 2007; published 20 December 2007)

Recently, strong reduction of the quasiparticle peaks and pronounced incoherent structures have been observed in the photoemission spectra of layered cobaltates. Surprisingly, these many-body effects are found to increase near the band-insulator regime. We explain these unexpected observations in terms of a novel spin-polaron model for CoO₂ planes, which is based on a fact of the spin-state quasidegeneracy of Co³⁺ ions in oxides. Scattering of the photoholes on spin-state fluctuations suppresses their coherent motion. The observed “peak-dip-hump” type line shapes are well reproduced by the theory.

DOI: 10.1103/PhysRevLett.99.256406

PACS numbers: 71.27.+a, 72.10.Di, 79.60.-i

Strongly correlated behavior of electrons is a common property of transition metal oxides. This is because the bandwidth is relatively small compared to the intraionic Coulomb repulsion between the 3*d* electrons. As a result, the celebrated Mott physics [1] forms a basis for understanding the unique properties of oxides, such as the high-*T_c* superconductivity and a colossal magnetoresistivity.

Recently, attention has focused on the layered cobalt oxides because they exhibit high thermoelectric power [2], i.e., the capability to transform heat energy into electricity. These compounds consist of triangular lattice CoO₂ planes, separated either by Na layers as in NaCoO₂ [3] or by BiO-BaO layers of rock-salt structure in so-called “misfit” cobaltates (see [4,5], and references therein). Besides controlling the *c*-axis transport, the Na and BiO-BaO layers introduce also the charge carriers into the CoO₂ planes, such that the valence state of Co ions is varied in a wide range from nonmagnetic Co³⁺ *t*_{2*g*}⁶ *S* = 0 state (as in NaCoO₂) towards the magnetic Co⁴⁺ *t*_{2*g*}⁵ *S* = 1/2 configuration (i.e., in Na_{*x*}CoO₂ at small *x*).

As the *t*_{2*g*}⁶ shell of Co³⁺ is full, this limit is naturally referred to as a band insulator [6,7], while Co⁴⁺ *S* = 1/2 rich compounds fall into the category of Mott systems because of unquenched spins. It has therefore been thought that layered cobaltates may provide an interesting opportunity to monitor the evolution of electronic states from a weakly correlated band-insulator regime to the strongly correlated Mott limit by hole doping of NaCoO₂ and misfits. Surprisingly, a completely opposite trend is found experimentally. The hallmarks of strong correlations such as magnetic order [3,8], strong magnetic field effects [2], etc., are most pronounced closer to the Co³⁺ compositions, while Co⁴⁺ *S* = 1/2 rich compounds behave as moderately correlated metals [3,9]. The best thermoelectric performance is also realized near the doped band-insulator regime [4,10]; thus unusual correlations and enhanced thermopower are clearly interrelated. As direct evidence of a complex structure of doped holes, the angular resolved

photoemission (ARPES) experiments [5,11] observed line shapes typical for strongly correlated systems. Paradoxically again, the many-body effects in ARPES are enhanced approaching the band-insulator limit [5].

This Letter presents a theory resolving this puzzling situation in layered cobaltates. We show that holes doped into nonmagnetic band insulators NaCoO₂ and misfits are indeed composite objects with a broad energy-momentum distribution of their spectral functions. Besides reduced quasiparticle peaks, they display also a dispersive incoherent structure as observed [5,11]. The physics behind this unexpected complexity is based on a unique aspect of Co³⁺ ions, i.e., their spin-state quasidegeneracy, and on special lattice geometry of CoO₂ layers.

In oxides, Co²⁺ is always in a high-spin 3/2 state while Co⁴⁺ ions usually adopt a low-spin 1/2. Roughly, this selection is decided by the Hund coupling favoring high-spin values or by the *t*_{2*g*}-*e_g* crystal field splitting 10*D_q* supporting low-spin states. An intermediate case is realized for Co³⁺ where the *S* = 0, 1, 2 states compete. This leads to a distinct property Co³⁺ rich oxides called “spin-state-transition” responsible for many anomalies such as spin-state changes in LaCoO₃ [12,13], and a spin-blockade effect in HoBaCo₂O_{5.5} [14], to mention a few manifestations of the Janus-like behavior of Co³⁺.

A new situation encountered in layered cobaltates is that CoO₆ octahedra are edge shared. In this geometry, the charge transfer occurs along the 90° Co-O-Co bonds, where the largest matrix element is that between the orbitals of *t*_{2*g*} and *e_g* symmetry (see \tilde{t} process in Fig. 1). This implies that a doped hole dynamically creates *S* = 1 *t*_{2*g*}⁵*e_g*¹ states of Co³⁺ [15]. It is this point where the holes—doped into an initially nonmagnetic background—become many-body objects dressed by virtual spin excitations. Formation of spin polarons suppresses the plane-wave-like motion of holes. However, they gain in the kinetic energy by exploiting the \tilde{t} hopping channel.

The layered structure of cobaltates results in quasi-two-dimensional electronic states as in cuprates. This should

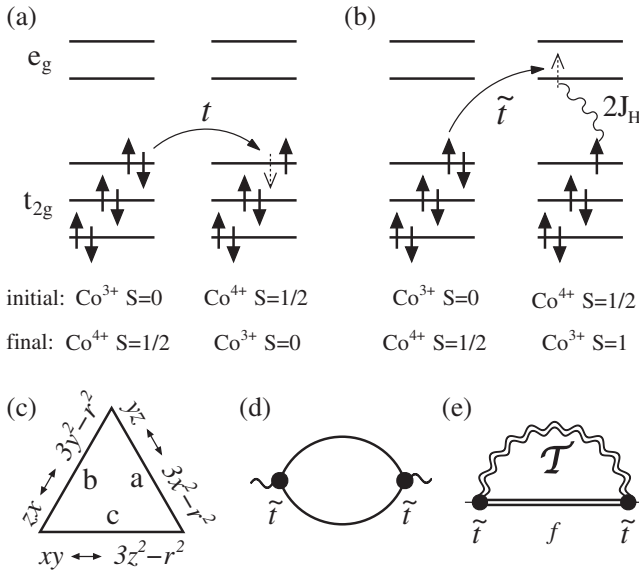


FIG. 1. (a) A conventional t hopping within the low-spin t_{2g} states. (b) \tilde{t} -hopping process creating an excited Co^{3+} $S = 1$ state. Because of the Hund coupling J_H , this state is quasidegenerate to the t_{2g}^6 $S = 0$ state; i.e., the excitation energy $E_T \sim 10Dq - 2J_H$ is low. In terms of Eq. (1), a fermionic hole moves to the left leaving behind \mathcal{T} excitation. (c) Bond directions a , b , and c in the triangular lattice of Co ions and \tilde{t} -coupled orbitals on these bonds. (d) Self-energy of the \mathcal{T} excitation. (e) Self-energy of the holes in a self-consistent Born approximation.

also lower the symmetry of the t_{2g} bands (threefold degenerate in the case of a cubic lattice) that accommodate doped holes. Indeed, ARPES data show a very simple Fermi surface derived from a single band of a_{1g} symmetry [5, 11]. This band can be described by the nearest-neighbor Hamiltonian $H_t = -t \sum_{ij\sigma} f_{j\sigma}^\dagger f_{i\sigma}$, where the fermionic operators f represent a_{1g} holes. They are subject to a conventional Gutzwiller constraint (at most one hole at a given site) but this is not much relevant at small density of holes, i.e., near the band-insulator limit. Hence, holes move freely as in a semiconductor.

In contrast, the t_{2g} - e_g hopping in Fig. 1(b) represents the many-body process as it produces the Co^{3+} $S = 1$ excitation. The model describing this process has been derived in Ref. [16] and reads as follows:

$$H_{\tilde{t}} = -\frac{\tilde{t}}{\sqrt{3}} \sum_{ij} [\mathcal{T}_{+1,\gamma}^\dagger(i) f_{j\ell}^\dagger f_{i\ell} - \mathcal{T}_{-1,\gamma}^\dagger(i) f_{j\ell}^\dagger f_{i\ell} - \mathcal{T}_{0,\gamma}^\dagger(i) \frac{1}{\sqrt{2}} (f_{j\ell}^\dagger f_{i\ell} - f_{j\ell}^\dagger f_{i\ell}) + \text{H.c.}] \quad (1)$$

Here, \mathcal{T} is the spin-triplet excitation generated by hopping of an electron from Co_j^{3+} to the e_g level of Co_i^{4+} (described as hole motion). The process, of course, conserves the total spin. In addition, the direction γ of the bond $\langle ij \rangle$ selects the e_g orbital involved in the \tilde{t} process [see Fig. 1(c)], accord-

ing to E_g symmetry relations between \mathcal{T}_γ operators:

$$\mathcal{T}_c = \mathcal{T}_{3z^2-r^2}, \quad \mathcal{T}_{a/b} = -\frac{1}{2} \mathcal{T}_{3z^2-r^2} \pm \frac{\sqrt{3}}{2} \mathcal{T}_{x^2-y^2}.$$

Based on this model, we develop a theory for the photoemission experiments in cobaltates. It is evident from (1) that by creating and destroying \mathcal{T} excitations as they propagate, the holes are strongly renormalized and we deal with a spin-polaron problem. This resembles the problem of doped Mott insulators like cuprates; however, the nature of spin excitations is different here because of the nonmagnetic ground state. Instead of magnonlike propagating modes as in cuprates, fluctuations of the very spin value of Co^{3+} ions are the cause of the spin-polaron physics in cobaltates [17].

For the calculation of the fermionic self-energies, we employ the self-consistent Born approximation [see Fig. 1(e)], which has extensively been used in the context of spin polarons in cuprates [21]. First, we focus on the spin-excitation spectrum. Since a direct e_g - e_g hopping in case of 90° bonds is not allowed by symmetry, the bare \mathcal{T} spin excitation is a purely local mode, at the energy E_T . The coupling to the holes in (1) shifts and broadens this level. Accounting for this effect perturbatively [see Fig. 1(d)], we obtain the \mathcal{T} Green's function $\mathcal{D}^{-1}(i\omega) = i\omega - E_T - \Sigma_T(i\omega)$ with

$$\Sigma_T(i\omega) = \frac{2\tilde{t}^2}{3\beta} \sum_{\mathbf{k}\mathbf{k}',i\epsilon} \Gamma_{\mathbf{k}} \mathcal{G}_0(\mathbf{k}, i\epsilon) \mathcal{G}_0(\mathbf{k}', i\epsilon + i\omega). \quad (2)$$

Here, \mathcal{G}_0 is the bare electron propagator $\mathcal{G}_0(\mathbf{k}, i\epsilon) = (i\epsilon - \xi_{\mathbf{k}})^{-1}$ with the a_{1g} dispersion on a triangular lattice $\xi_{\mathbf{k}} = -2t(c_a + c_b + c_c) + \mu$, where $c_\gamma = \cos k_\gamma$ and k_γ are the projections of \mathbf{k} on a , b , and c directions. The underlying E_g symmetry of \mathcal{T} operators involved in \tilde{t} hopping results in the factor $\Gamma_{\mathbf{k}} = c_a^2 + c_b^2 + c_c^2 - c_a c_b - c_b c_c - c_c c_a$. We neglected a weak momentum dependence of Σ_T for the sake of simplicity. This is justified as long as Σ_T is small compared to the spin gap E_T .

Further, we approximate $\Gamma_{\mathbf{k}}$ by its Brillouin-zone average $3/2$, obtaining the simple expressions for Σ_T in terms of bare fermionic density of states $N_0(x) = \sum_{\mathbf{k}} \delta(x - \xi_{\mathbf{k}})$:

$$\text{Im} \Sigma_T(E) = -\pi \tilde{t}^2 \int_{-E}^0 dx N_0(x) N_0(x + E), \quad (3)$$

$$\text{Re} \Sigma_T(E) = -\tilde{t}^2 \int_{-\infty}^0 dx \int_{x^2}^{\infty} dy^2 \frac{N_0(x) N_0(x + y)}{y^2 - E^2}. \quad (4)$$

These equations determine the renormalized spin-excitation spectrum $\rho_T(E) = -\pi^{-1} \text{Im} \mathcal{D}(i\omega \rightarrow E + i\delta)$ used below for calculation of the fermionic self-energy.

The self-energy diagram in Fig. 1(e) reads as

$$\Sigma_{\mathbf{k}}(i\epsilon) = -\frac{2\tilde{t}^2}{\beta} \sum_{\mathbf{k}',i\omega} [\Gamma_{\mathbf{k}'} \mathcal{D}(-i\omega) + \Gamma_{\mathbf{k}} \mathcal{D}(i\omega)] \times \mathcal{G}(\mathbf{k}', i\epsilon + i\omega), \quad (5)$$

where $\mathcal{G}^{-1}(\mathbf{k}, i\epsilon) = i\epsilon - \xi_{\mathbf{k}} - \Sigma_{\mathbf{k}}(i\epsilon)$. We can write

$\Sigma_{\mathbf{k}}(\omega) = 2\tilde{t}^2[\Phi(\omega) + \Gamma_{\mathbf{k}}\Xi(\omega)]$, where

$$\Phi(\omega) = \int_0^\infty dE \rho_T(E) \int_0^\infty dx \frac{\tilde{N}(x)}{\omega - E - x + i\delta}, \quad (6)$$

$$\Xi(\omega) = \int_0^\infty dE \rho_T(E) \int_{-\infty}^0 dx \frac{N(x)}{\omega + E - x + i\delta}. \quad (7)$$

The full local density of states $N(E) = \sum_{\mathbf{k}} A(\mathbf{k}, E)$ and its E_g symmetry part $\tilde{N}(E) = \sum_{\mathbf{k}} \Gamma_{\mathbf{k}} A(\mathbf{k}, E)$ are functions of the self-energy itself, via the spectral functions $A(\mathbf{k}, E) = -\pi^{-1} \text{Im} \mathcal{G}(i\epsilon \rightarrow E + i\delta)$. The above equations are thus to be solved self-consistently.

Next, we test the reliability of approximations made. To this end, we performed an exact diagonalization of our model $H = H_t + H_{\tilde{t}}$ on a $\sqrt{7} \times \sqrt{7}$ hexagonal cluster [Fig. 2(d)]. We inject one hole on such a cluster and calculate its spectral function

$$A(\mathbf{k}, E) = -\frac{1}{\pi} \text{Im} \langle \text{GS} | f_{\mathbf{k},\sigma}(z - H)^{-1} f_{\mathbf{k},\sigma}^\dagger | \text{GS} \rangle, \quad (8)$$

where $z = E + E_{\text{GS}} + i\delta$. Since the ground state |GS> contains no holes and the single hole on the cluster represents 1/7 doping, the effective doping is about 10%. Periodic boundary conditions allow us to access two non-equivalent \mathbf{k} points [see Fig. 2(d)]. To obtain continuous profiles of $A(\mathbf{k}, E)$, we broaden the excited states.

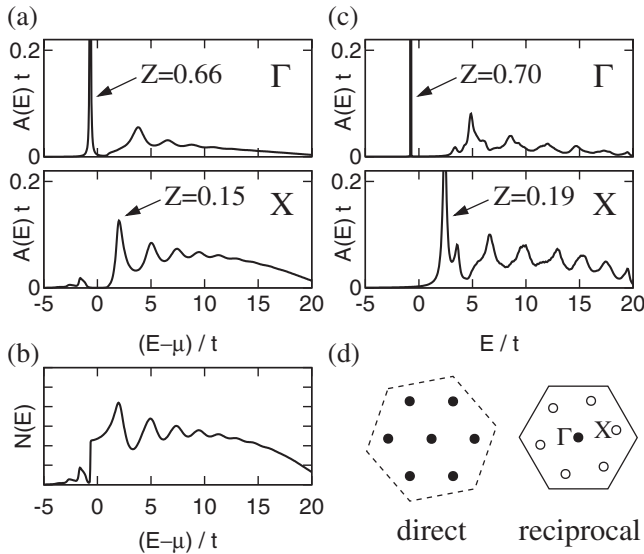


FIG. 2. Comparison of the analytical results at 10% doping (left) and from exact diagonalization (right). (a) Spectral functions and a quasiparticle weight Z obtained from Eqs. (2) and (5) with bare $E_T = 1.2t$ (renormalized to $\tilde{E}_T/t \approx 1$ by interactions) and (b) the corresponding density of states $N(E)$. The incoherent structure dominates $N(E)$. A peak around $2t$ corresponds to the van Hove singularity smeared by interaction effects. (c) Spectral functions from exact diagonalization at $E_T/t = 1$. (d) The 7-site cluster in direct space (the dashed line defines the supercell) and in reciprocal space (full line is the Brillouin zone boundary). The allowed $\mathbf{k} = \Gamma, X$ points are indicated by \bullet and \circ .

Our model has two parameters: \tilde{t}/t and E_T/t . In fact, the ratio $\tilde{t}/t \approx 3$ follows from the relations $t = 2t_0/3$ and $\tilde{t}/t_0 = t_\sigma/t_\pi \approx 2$ (where $t_0 = t_\pi t_\pi/\Delta_{\text{pd}}$) [16]. Thus, we set below $\tilde{t}/t = 3$, leaving E_T as a free parameter.

We find that the above equations give results consistent with the exact diagonalization, even at rather small spin gap values $E_T \sim t$, as shown in Figs. 2(a) and 2(c). Both approaches lead to spectral functions with a renormalized quasiparticle (qp) peak whose spectral weight is transferred to a pronounced hump structure. [A peculiar momentum dependence of the matrix elements $\Gamma_{\mathbf{k}}$ (note that $\Gamma_{\mathbf{k}=0} = 0$) reduces the effect at $\mathbf{k} = \Gamma$ point.] Several maxima on the hump reflect the presence of multiple triplet excitations created by the hole propagation. All these are the typical signatures of polaron physics. The multiplet structure of the hump will in reality be smeared by phonons that are naturally coupled to the \tilde{t} transition involving also the orbital sector. Although experiments [22] indicate that electron-phonon coupling is moderate in cobaltates, it may enhance the spin-polaron effects as in cuprates [23].

To illustrate the gross features of the hole renormalization, in Fig. 3 we show a complete map of the spectral function along the M - Γ - K path in the Brillouin zone. We have used a representative value $E_T = 2t$, which is renormalized by holes to $\tilde{E}_T \approx 1.4t$. Compared to the bare dispersion, the bandwidth of the renormalized holes is reduced by a factor of ~ 2 . The main observation here is that as the hole energy reaches \tilde{E}_T , the dynamical genera-

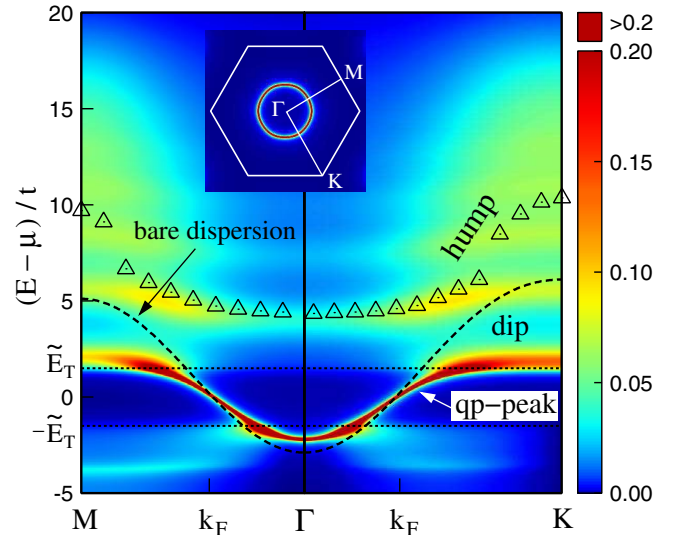


FIG. 3 (color online). Intensity map of the spectral density $A(\mathbf{k}, E)$ of the Co^{4+} holes along the M - Γ - K path in the Brillouin zone calculated at 30% doping and $E_T = 2t$. As the hole energy reaches the renormalized spin-excitation energy \tilde{E}_T , the qp peak broadens and its weight is transferred to a broad, incoherent structure. This results in a “peak-dip-hump” profile of $A(\mathbf{k}, E)$ seen also in Fig. 2. The top of the smoothed hump structure is indicated by triangles. The dashed line shows the bare dispersion. The Fermi surface is shown in the inset.

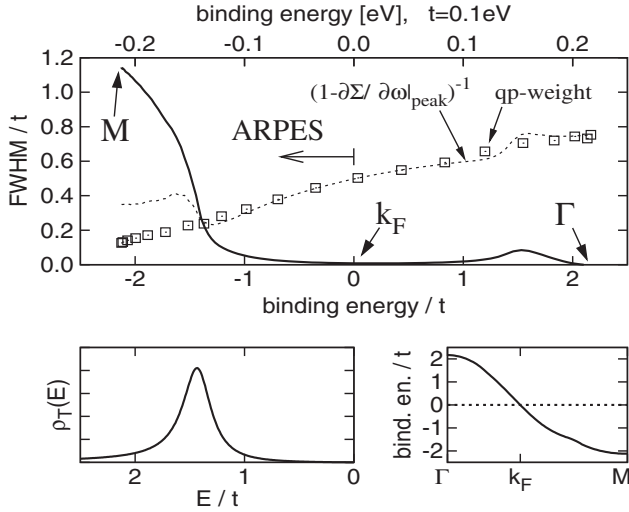


FIG. 4. Top panel: Full energy width at half maximum of the quasiparticle peak along the M - Γ dispersion curve (see bottom-right panel) plotted as a function of the binding energy. The part from k_F to M is accessible by ARPES experiments. Strong qp damping below $\sim -1.4t$ is due to a scattering on $S = 1$ excitations. The spectral weight of the qp peak obtained by a direct integration is indicated by squares. When damping is small, it coincides with a conventional qp residue $(1 - \partial\Sigma'/\partial\omega)^{-1}$. Lower panel: The \mathcal{T} -exciton spectral function (left), and renormalized hole dispersion (right).

tion of $S = 1$ excitations becomes very intense and a broad incoherent response develops, leading to the pronounced “peak-dip-hump” structure of $A(\mathbf{k}, E)$. Following the maximum of the smoothed hump structure, we observe its strong dispersion (stemming also from incoherent \tilde{t} hopping).

Figure 3 suggests a possible determination of \tilde{E}_T from the quasiparticle damping. To address this problem, in Fig. 4 we show the energy width of the qp peak following its dispersion curve. The sharp onset of the damping at the binding energy $\approx -1.4t$ is clearly related to the maximum of the spin-excitation spectral function $\rho_T(E)$. In addition, Fig. 4 shows the weight of the qp peak, which is \mathbf{k} dependent (mainly due to the matrix element $\Gamma_{\mathbf{k}}$).

Comparison of Figs. 3 and 4 with the data of Refs. [5,11] reveals a remarkable correspondence between theory and experiment. In particular, both the qp peak and the hump dispersions (see Figs. 2 and 3 of Ref. [5]) are well reproduced by theory, considering $t \approx 0.1$ eV suggested by the band structure fit [24]. The onset energy $\tilde{E}_T \sim 1.4t$ for the qp damping (Fig. 4) is then ≈ 0.14 eV, in agreement with experiment [see Fig. 2(c) of Ref. [5]]. Physically, dilute spin polarons are expected to be pinned by disorder, thus qp peaks should be suppressed at low hole doping.

To summarize, we have presented a theory for the photoemission experiments in layered cobaltates. A strong damping of quasiparticles, their reduced spectral weights,

broad and dispersive incoherent structures, and “peak-dip-hump” type line shapes all find a coherent explanation within our model. We thus conclude that unusual correlations observed near the band-insulator regime are the direct manifestation of the spin-state quasidegeneracy of Co ions, and this intrinsic feature of cobaltates should be the key for understanding their unique properties, such as the high thermopower. In particular, the spin-polaronic nature of holes should be essential for explanation of its remarkable magnetic field sensitivity [2].

We thank B. Keimer for stimulating discussions. This work was partially supported by the Ministry of Education of CR (No. MSM0021622410).

- [1] N.F. Mott, *Metal-Insulator Transitions* (Taylor and Francis, London, 1974).
- [2] Y. Wang, N. S. Rogado, R. J. Cava, and N. P. Ong, *Nature (London)* **423**, 425 (2003).
- [3] M. L. Foo *et al.*, *Phys. Rev. Lett.* **92**, 247001 (2004).
- [4] J. Bobroff *et al.*, *Phys. Rev. B* **76**, 100407(R) (2007).
- [5] V. Brouet *et al.*, *Phys. Rev. B* **76**, 100403(R) (2007).
- [6] G. Lang *et al.*, *Phys. Rev. B* **72**, 094404 (2005).
- [7] C. de Vaulx *et al.*, *Phys. Rev. Lett.* **95**, 186405 (2005).
- [8] S. P. Bayrakci *et al.*, *Phys. Rev. Lett.* **94**, 157205 (2005).
- [9] C. de Vaulx *et al.*, *Phys. Rev. Lett.* **98**, 246402 (2007).
- [10] M. Lee *et al.*, *Nat. Mater.* **5**, 537 (2006).
- [11] D. Qian *et al.*, *Phys. Rev. Lett.* **97**, 186405 (2006).
- [12] M. W. Haverkort *et al.*, *Phys. Rev. Lett.* **97**, 176405 (2006).
- [13] S. Yamaguchi, Y. Okimoto, H. Taniguchi, and Y. Tokura, *Phys. Rev. B* **53**, R2926 (1996).
- [14] A. Maignan *et al.*, *Phys. Rev. Lett.* **93**, 026401 (2004).
- [15] $t_{2g}^4 e_g^2$ $S = 2$ configuration is not accessible by hopping.
- [16] G. Khaliullin and J. Chaloupka, arXiv:cond-mat/0707.2364.
- [17] In contrast to Refs. [18,19], where a *static* hole surrounded by $S = 1$ Co^{3+} ions was studied, in the present model the triplet $S = 1$ excitations are *virtual* and generated dynamically by the *very motion* of the hole via the \tilde{t} process. These two pictures can merge if a hole is strongly trapped (e.g., by Na potential [20]).
- [18] G. Khaliullin, *Prog. Theor. Phys. Suppl.* **160**, 155 (2005).
- [19] M. Daghofer, P. Horsch, and G. Khaliullin, *Phys. Rev. Lett.* **96**, 216404 (2006).
- [20] M. Roger *et al.*, *Nature (London)* **445**, 631 (2007).
- [21] See, e.g., C. L. Kane, P. A. Lee, and N. Read, *Phys. Rev. B* **39**, 6880 (1989).
- [22] J.-P. Rueff *et al.*, *Phys. Rev. B* **74**, 020504(R) (2006).
- [23] A. S. Mishchenko and N. Nagaosa, *Phys. Rev. Lett.* **93**, 036402 (2004); O. Rösch and O. Gunnarsson, *Phys. Rev. Lett.* **93**, 237001 (2004).
- [24] S. Zhou *et al.*, *Phys. Rev. Lett.* **94**, 206401 (2005), find the nearest-neighbor interorbital hopping $t' = -157.8$ meV. Projection to the a_{1g} -hole subband yields [16] $t = -2t'/3 \approx 0.1$ eV.